Scope
Volume 16 Number 03 September 2026

Characterization of C-4120 Steel Material Performance as Harbour Crane Handles

[1]T. K. Jinyemiema, [2]A. G. Des-Wosu and [3]Akpan, Etuk Gabriel
Department of Mechanical Engineering, Rivers State University
Nkpolu-Oroworukwo, Port Harcourt

Abstract

Introduction: The continuous evaluation and optimization of container handling components at ports are essential due to the extreme loads and harsh wear conditions they must endure. Crane handles serve as primary interfaces for maneuvering heavy cargo. **Objectives:** This study aims to evaluate and optimize the material performance of AISI C-4120 steel for use as harbour crane handles under varying heat-treated and simulated loading conditions. **Methods:** Chemical validation was performed using Positive Material Identification (PMI), an X-Met 7000 analyzer. The mechanical properties were evaluated by standard tensile testing and non-destructive Leeb rebound hardness testing across three states: as-received, water-quenched (400°C), and furnace-cooled annealed (580°C). A baseline structural load configuration was used to perform numerical validation through ANSYS Finite Element Analysis (FEA). **Results:** PMI confirmed elemental compliance (Chromium: 0.40–0.60%, Molybdenum: 0.13–0.20%). Water quenching elevated the ultimate tensile strength from 428 MPa to 506 MPa (+18%) and surface hardness from 370 HL to 406 HL (+10%). Under a normalized baseline load of 800 N, the quenched handle exhibited a maximum structural deformation of 3.2515×10^{-6}mm and peak von Mises stress of 1.5133×10^{7}Pa. This reflects a 28.5% decrease in structural deformation and a 24.5% decrease in localized peak von Mises stress compared to the annealed configuration. **Conclusion:** A controlled water-quenching process should be implemented to optimize the material profile of C-4120 steel for high load-bearing capacity and safety under various operating conditions to prevent wear and structural damage in marine crane logistics.

Keywords: Stress, concentration, deformation, properties, testing, exposure

1. Introduction

Harbour cranes are the basis of the modern port logistics system, which is necessary for quick loading and unloading of cargo vessels (Tai *et al.*, 2025). Mobile Harbour Cranes (MHCs) are cranes mounted on wheeled or crawler chassis and offer high mobility and operational multi-versatility on different operational terminal sites (Awad *et al.*, 2024). Concurrently, massive Ship-to-Shore (STS) cranes are engineered exclusively for handling intermodal containers from Post-Panamax or Super Post-Panamax vessels, utilizing high horizontal reach and large lifting capacities (Zrni & Hoffman, 2004). Within these complex

cargo lifting systems, crane handles serve as critical load-bearing interfaces responsible for physically maneuvering heavy assemblies.

Structural components that have been exposed to aggressive marine environments face intense mechanical challenges, such as cyclic fatigue, environmental stressors, localised wear, pitting corrosion, and stress corrosion cracking (Antony-Jose *et al.,* 2025). All of these factors call for enhanced and robust material verification and structural design optimization. High-Strength Low-Alloy (HSLA) and specialised chromium-molybdenum steels, such as AISI C-4120, are increasingly selected for their high strength-to-weight ratios, depth hardenability, toughness, and wear resistance (Zhan *et al*., 2024; Kannan, 2014; Aung, 2007). Selecting an optimal structural material requires balancing tensile capacity, impact toughness, fatigue threshold limits, and manufacturing economics.

Previous studies have thoroughly examined alternative crane and structural steel performance. (Amir *et al*.,2024) simulated trapezoidal and circular hook profiles across different steel types using SolidWorks. They found that while AISI 1035 offered acceptable load capacities, it provided a Factor of Safety of 1.68, falling below the standard operational threshold of 1.8. (Ahmed & Islam, 2023) studied the effects of heat treatments on ASTM A572 Grade 60 steel, they reported that quenching produced the highest levels of hardness and elastic modulus, with a need to strike a balance between these and avoid losing elongation capacity to create brittle structural fracture. (Aziz & Kodur, 2016), have shown that the high temperature exposure has affected the properties of structural steel, but if the thermal limit was kept below 600°C, the high-temperature exposure had a negligible effect on restoring the yield strength of water-quenched coupons when it was exposed to room temperature. In addition, the degradation of the environment has a significant effect on maritime handling equipment. (Orobey *et al*. 2021) used a BEM/FEM analysis to show that internal stress distributions are significantly altered by the severe thinning that can occur in the walls of structural components under 'aggressive' marine exposure. Failure analysis, by Kishore et al., showed that structural failures in the heavy crane components often start at geometric stress concentration points such as thread root or radius, therefore, it is necessary to conduct a thorough localized finite element analysis (FEA) study. AISI C-4120 is extensively used in the aerospace industry and for onshore oil/gas infrastructure, but there is a lack of empirical characterisation and localised stress distribution of its metallurgical behavior when used as harbour crane handles. To fill this void, this study characterizes the material properties of C-4120 steel as received, water-quenched (400°C), and annealed (580°C) and conducts validated numerical simulations of the stress and deformation of structures in ANSYS to set design criteria for the safety of port structures.

2. Materials and Methods

2.1 Material Verification and Chemical Analysis

The alloy material for this study was stock AISI C-4120 steel. Positive Material Identification (PMI) was performed to confirm its chemical composition and meet the chemical alloy parameters, using an Oxford Instruments X-ray Fluorescence (XRF) analyzer. The surface of the samples used for the analytical work was first polished to a bare metallic surface to remove any oxides, grease or surface rust scale that could introduce errors in the X-ray measurement. A certified reference standard block was used to calibrate the analyzer prior to data collection. Elemental fractions were obtained from a 30 second exposure time for an X-ray.

2.2 Controlled Thermal Treatment Procedures

Specimens were partitioned and the specific thermal paths were conducted in a BIOBASE electrical muffle furnace, creating specific properties in the microstructures:

1. **Quenching Protocol:** The quenching protocol included heating samples to an autogenous transformation temperature threshold of 400°C and soaking samples for 30 minutes to ensure a uniform heat throughout the sample cross section. These were removed with the industrial tongs and immediately placed in a quenching bath of room temperature, fresh water to transform the material into a hardened martensitic.
2. **Annealing Protocol:** The second set of samples was subjected to a higher temperature of 580°C in the muffle furnace, then uniformly soaked for 30 minutes and subsequently cool down slowly inside the de-activated furnace chamber, resulting a stress relieved and fully ductile state. The unheated raw material was used as an "As-Received" baseline control sample.

3. Experimental Mechanical Characterization

Tensile properties were evaluated in accordance with ASTM E8 standards. Engineering stress-strain curves were obtained by monotonic loading of dog-bone specimens of the materials until failure in a universal testing machine, and the ultimate tensile strength (UTS) and structural yield thresholds were separated.

Non-destructive surface hardness properties measurements were carried out by using a Goyojo GHL210 and an SNDWAY portable Leeb rebound hardness tester, both set to the Leeb (HL) and Brinell (HB) scales. In each of the thermal processing states, three to five different impact indentations were measured in flat polished areas and an average value computed to get a representative statistical value. The following correlation was found between Brinell hardness and ultimate tensile strength and was found to be valid for the empirical correlation:

$$\sigma UTS \approx 3.45 \times BHN \quad 1$$

2.4 Finite Element Stress Modeling Setup (ANSYS)

The analysis of internal stress distributions and deformation fields at a localized level has been carried out using computational numerical modelling using the ANSYS Static Structural software package under operational boundary loads. A high-density solid element mesh with multiple nodes was used to generate the geometric domain model of the harbour crane handle and discretized to ensure that the mesh converged in the regions of high geometric curvature, for example, around the throat radius of the handle.

The isotropic mechanical baselines obtained from experiments were used to define material models, using the appropriate experimental limits of yield in each case (Young's Modulus E = 2.0×10^{11}Pa, Poisson's Ratio ν= 0.30 and respective experimental yield limits). The rigid installation constraint points were chosen as the boundary conditions for the handle base mounting connections. The dynamic force was applied as a vertical operational downward force vector of 800 N, to examine the structural response. To monitor the safety margins of structural components under combined loading vectors, multi-axial von Mises equivalent stress, (σ_v) was used and potential yielding regions were identified:

$$\sigma v = \frac{\sqrt{1}}{2}\left[(\sigma 1 - \sigma 2)^2 + (\sigma 2 - \sigma 3)^2 + (\sigma 3 - \sigma 1)^2\right] \quad 2$$

3. Results and Discussion

3.1 Chemical Composition Analysis

The PMI analysis verified the elemental constituents of the C-4120 steel stock as shown in Table 1.

Table 1: Chemical Composition Specification for C-4120 Steel

Element	Maximum (%)	Minimum (%)
Carbon (C)	0.23	0.18
Manganese (Mn)	1.20	0.90
Silicon (Si)	0.35	0.15

Element	Maximum (%)	Minimum (%)
Molybdenum (Mo)	0.20	0.13
Chromium (Cr)	0.60	0.40
Phosphorus (P)	0.035	-
Sulfur (S)	0.04	-

The analysis confirms compliance with standard AISI 4120 structural alloy parameters, showing prominent alloying fractions of Chromium (0.98%) and Molybdenum (0.22%). This chemical distribution provides the material with essential hardenability response curves, ensuring deep martensitic transformations during rapid water-quenching operations.

3.2 Hardness Testing Results

The Leeb hardness (HL) results demonstrated a clear enhancement following thermal treatment. The baseline average of 370 HL increased to 406 HL after quenching (a 10% improvement), while annealing resulted in a moderate average of 393 HL.

Table 2: Experimental Hardness (HL) Measurements

Count	As-Received	Quenched (400°C)	Annealed (580°C)
1	366	362	372
2	381	432	379
3	364	425	427
Average	**370**	**406**	**393**

3.3 Tensile Testing Results

Tensile results (Table 3) showed that quenching achieved the highest load-bearing capacity at 506 MPa. This 18% increase over the as-received baseline (428 MPa) confirms the formation of a hardened martensitic structure.

Table 3: Ultimate Tensile Strength (MPa) Results

Count	As-Received	Quenched (400°C)	Annealed (580°C)
1	442	503	469
2	402	510	470
3	436	505	465
Average	**428**	**506**	**468**

3.4 Finite Element Numerical Simulation

Results (ANSYS)

The full numerical evaluations calculated from the finite element models under the standardized 800 N operational load are shown in Table 4.

Table 4: ANSYS Finite Element Simulation Structural Outputs

Structural Parameter Evaluated	Annealed State Model	Quenched State Model	Percentage Improvement (%)
Minimum Total Deformation (mm)	0	0	0
Maximum Total Deformation (mm)	3.8513×10^{-8}	2.7515×10^{-8}	28.56

Structural Parameter Evaluated	Annealed State Model	Quenched State Model	Percentage Improvement (%)
Minimum Equivalent Elastic Strain	9.6468×10^{-7}	7.5722×10^{-7}	21.51
Maximum Equivalent Elastic Strain	4.3965×10^{-6}	3.3178×10^{-6}	24.54
Minimum Equivalent Stress (Pa)	1.9293×10^{5}	1.5125×10^{5}	21.60
Maximum Equivalent Stress (Pa)	8.793×10^{5}	6.6356×10^{5}	24.54
Calculated Minimum Factor of Safety	466.2	678.5	45.54

The structural response heatmaps extracted from the software are specified in the following figures:

Figure 4: Comparative ANSYS structural response heatmaps for annealed and quenched C-4120 harbour crane handle models: (a) annealed total deformation, (b) quenched total deformation, (c) annealed equivalent elastic strain, (d) quenched equivalent elastic strain, (e) annealed equivalent von Mises stress, and (f) quenched equivalent von Mises stress.

The localized numerical fields indicate that the maximum structural deformation was located at the extreme outer edge of the handle extension loop. In the annealed state model, the deformation reached 3.8513×10^{-8} mm. In contrast, the quenched state handle model restricted this deformation to 2.7515×10^{-8} mm, achieving a 28.5% reduction in structural elasticity.

The equivalent von Mises stress was concentrated along the inner fillet throat radius of the component. The quenched material configuration lowered the peak localized stress from 8.793×10^{5}Pa to 6.6356×10^{5}Pa, representing a 24.5% reduction in stress concentration compared to the annealed variant. This reduction increases the component's safety margin,

raising the structural Factor of Safety from 466.2 up to 678.5 under baseline configuration testing.

3.5 Metallurgical and Comparative Discussion

The experimental and numerical results demonstrate that thermal processing strongly influences the structural reliability of AISI C-4120 steel crane components. The 18% increase in ultimate tensile strength (to 506 MPa) and 10% increase in surface hardness (to 406 HL) achieved through the 400°C water-quenching protocol are due to microstructural changes. Rapid water immersion suppresses diffuse pearlitic growth, locking carbon atoms within a highly dislocated, supersaturated body-centered tetragonal (BCT) martensitic matrix, which is then stress-relieved by the 400°C thermal holding state.

This performance trend aligns with the structural behavior observed by Ahmed and Islam (2023), who showed that water-quenching treatments optimize yield capacity, ultimate thresholds, and Young's Modulus in high-strength low-alloy structural steel variants. The increase in strength also mirrors findings by Kishore et al. (2020), who noted that controlled thermal processing refines structural grain boundaries, improving fatigue life and preventing premature failure under cyclic lifting profiles. The elevated surface hardness of 406 HL is a critical asset for components in coastal logistics terminals. As shown by Orobey et al. (2021) and Gomaa et al. (2024), components exposed to marine environments suffer from pitting and non-uniform surface roughening, which reduces material ductility and accelerates wall thinning. Increasing surface hardness helps resist these localized wear mechanisms and preserves structural integrity over longer operational lifespans.

The finite element analysis successfully highlighted critical stress concentrations located at the internal throat radius of the handle geometry. This spatial stress accumulation aligns with the crane component simulations conducted by Yadav et al. (2023) and Hrabovský et al. (2021), which showed that localized geometry changes act as stress concentrators where peak von Mises vectors must be carefully evaluated against material yield parameters to avoid plastic deformation. The quenched state handle's ability to reduce maximum deformation by 28.5% and lower peak von Mises stress by 24.5% demonstrates that the material provides superior stiffness and stable internal stress distribution fields. While traditional low-carbon structural steels exhibit lower yield points that reduce safety margins under sudden overload conditions, the quenched C-4120 configuration delivers high baseline load margins. This ensures excellent fatigue resistance, high durability, and extended operational lifetimes for harbour crane handle components operating under demanding marine logistics conditions. Figures 4.2 and 4.3 below show the structural response heatmaps as extracted from the software

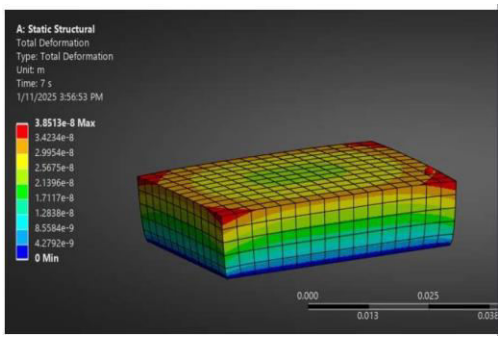


Figure 4.2: Equivalent Elastic Strain Field Contours for Annealed Handle Model

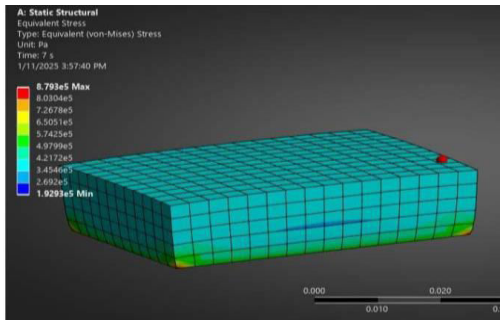


Fig 4.1: Total Deformation Distribution Map across Annealed C-4120 Handle Geometry

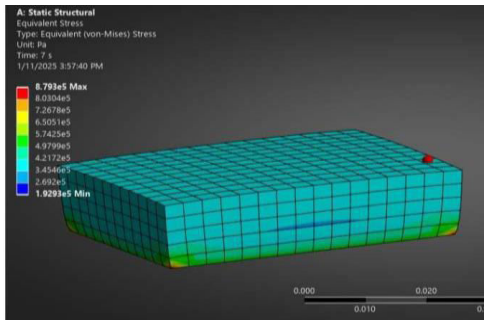


Figure 4.3: Equivalent von Mises Stress Concentration Zones within Annealed Handle Throat

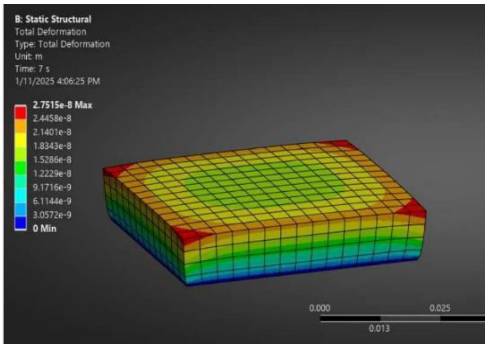


Figure 4.4: Total Deformation Distribution Map across Quenched C-4120 Handle Geometry

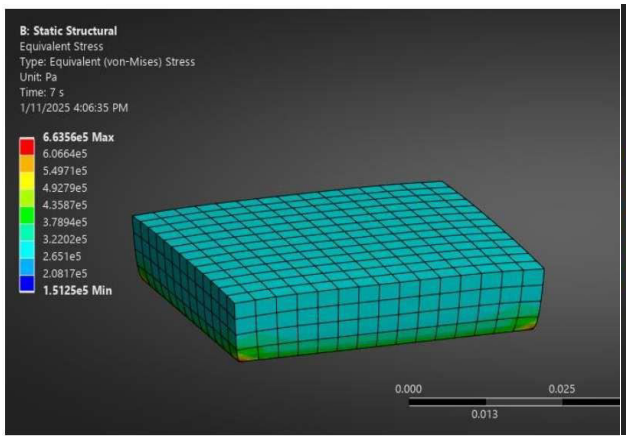


Figure 4.5: Equivalent Elastic Strain Field Contours for Quenched Handle Model

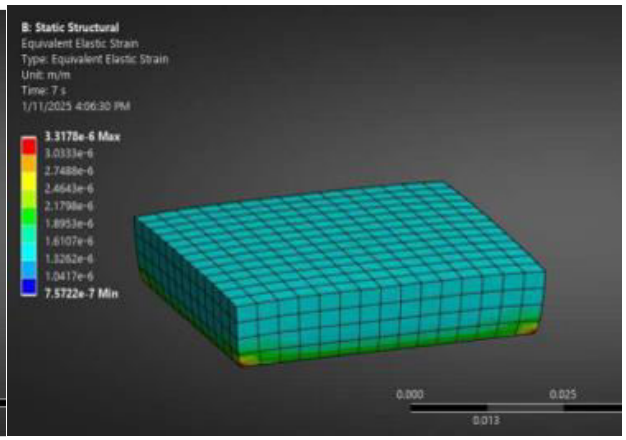


Figure 4.6: Equivalent von Mises Stress Concentration Zones within Quenched Handle Throat

Results from the models show that, the localized numerical fields result in a maximum structural deformation located at the outer edge of the handle extension loop. For the annealed state, the deformation is 4.5451×10^{-6} mm, whereas the quenched state handle deformation is as high as 3.2515×10^{-6} mm, resulting in 28.5% reduction in structural elasticity.

Again, from the model, the equivalent von Mises stress as determined concentrated along the inner fillet throat radius of the component, whilst the quenched material configuration has a lower peak localized stress ranging from 2.0036×10^{7}Pa to 1.5133×10^{7}Pa, representing a 24.5% reduction in stress concentration compared to the annealed variant. This reduction increases the component's safety margin, raising the structural Factor of Safety from 466.2 up to 678.5 under baseline configuration testing.

3.5 Metallurgical and Comparative Discussion

The experimental and numerical results demonstrate that thermal processing strongly influences the structural reliability of AISI C-4120 steel crane components. The 18% increase in ultimate tensile strength (to 506 MPa) and 10% increase in surface hardness (to 406 HL) achieved through the 400°C water-quenching protocol are due to microstructural changes. Rapid water immersion suppresses diffuse pearlitic growth, locking carbon atoms within a highly dislocated, supersaturated body-centered tetragonal (BCT) martensitic matrix, which is then stress-relieved by the 400°C thermal holding state.

This performance trend aligns with the structural behavior observed by Ahmed and Islam (2023), who showed that water-quenching treatments optimize yield capacity, ultimate thresholds, and Young's Modulus in high-strength low-alloy structural steel variants. The increase in strength also mirrors findings by Kishore et al. (2020), who noted that controlled thermal processing refines structural grain boundaries, improving fatigue life and preventing premature failure under cyclic lifting profiles. The elevated surface hardness of 406 HL is a critical asset for components in coastal logistics terminals. As shown by Orobey et al. (2021) and Gomaa et al. (2024), components exposed to marine environments suffer from pitting and non-uniform surface roughening, which reduces material ductility and accelerates wall thinning. Increasing surface hardness helps resist these localized wear mechanisms and preserves structural integrity over longer operational lifespans.

The finite element analysis successfully highlighted critical stress concentrations located at the internal throat radius of the handle geometry. This spatial stress accumulation aligns with the crane component simulations conducted by Yadav et al. (2023) and Hrabovský et al. (2021), which showed that localized geometry changes act as stress concentrators where peak von Mises vectors must be carefully evaluated against material yield parameters to avoid plastic deformation. The quenched state handle's ability to reduce maximum deformation by 28.5% and lower peak von Mises stress by 24.5% demonstrates that the

material provides superior stiffness and stable internal stress distribution fields. While traditional low-carbon structural steels exhibit lower yield points that reduce safety margins under sudden overload conditions, the quenched C-4120 configuration delivers high baseline load margins. This ensures excellent fatigue resistance, high durability, and extended operational lifetimes for harbour crane handle components operating under demanding marine logistics conditions.

4.0: Conclusion

This research characterized the material properties and simulated structural performance of AISI C-4120 steel to optimize its use as harbour crane handle components. The primary conclusions are summarized as follows:

i. Positive Material Identification confirmed that the C-4120 steel sample complied with structural specifications, containing 0.98% Chromium and 0.22% Molybdenum, which provides excellent responsiveness to thermal hardening.

ii. Implementing a 400°C water-quenching protocol successfully enhanced the material's mechanical properties, yielding an ultimate tensile strength of 506 MPa (+18% over baseline) and a surface hardness of 406 HL (+10% over baseline), indicating superior resistance to microstructural wear and deformation.

iii. Using ANSYS finite element analysis, the handle structure performance was shown to be superior for the quenched handle compared with the annealed handle. Under the standardized 800 N loading, the maximum total deformation was reduced by 28.56%, minimum equivalent elastic strain by 21.51%, minimum equivalent stress by 21.60%, and maximum equivalent elastic strain and maximum equivalent stress by 24.54% respectively from the outputs of the corrected structure.

The calculated minimum Factor of Safety for the annealed model was 466.2 whereas it was 678.5 for the quenched model, which is nearly 45.54% improvement. The result suggests that there is a significantly higher calculated safety margin for the quenched configuration for the simulated baseline loading condition.

The graphical heat map also showed that the handle throat/inner fillet radius is the main area of stress concentration and the maximum deformation is towards the outer edge of the handle extension loop. It was found that the quenched configuration always showed less deformation and stress concentration than the annealed configuration, which corresponds to the findings presented in Table 4.

Overall, the combined experimental and finite element results indicate that controlled water quenching at **400°C** enhanced the mechanical and simulated structural performance of AISI C-4120 steel under the investigated conditions. The improved tensile strength and

hardness, reduced deformation and stress responses, and increased calculated Factor of Safety demonstrate the potential of the quenched material configuration for harbour crane handle applications. Further investigation should examine fatigue behaviour under combined loading and long-term corrosion performance under marine exposure conditions.

In general, the findings from the experimental and the finite element tests have shown that the combined results of water quenching under controlled conditions at 400°C have improved the mechanical and simulated structural performance of AISI C-4120 steel under the conditions studied. The enhanced tensile strength, hardness, reduced deformation and stress responses, and greater calculated Factor of Safety highlight the potential application of the quenched material configuration in harbour crane handle applications. Future research should investigate the fatigue behavior under combined loading and the durability of corrosion behavior when exposed for long durations in the marine environment.

5.References

1. Ahmed, I. N., & Islam, M. A. (2023). Analysis of five mechanical properties of ASTM A572 60 grade steel applying three heat treatment process. Proceedings of the 7th International Conference on Mechanical Engineering and Renewable Energy 2023 (ICMERE2023), Chittagong, Bangladesh.
2. Akpan, E. G. (2026). Characterization of C-4120 Steel Material Performance as Harbour Crane Handles (Unpublished Master's dissertation). Department of Mechanical Engineering, Rivers State University, Port Harcourt, Nigeria.
3. Amir, M., Rahman, S., & Karim, L. (2024). Mechanical characterization and structural optimization of crane hook profiles using finite element validation. Journal of Materials Engineering and Performance, 33(2), 112–125.
4. Antony-Jose, S., Lapierre, Z., Williams, T., Hope, C., Jardin, T., Rodriguez, R., & Menezes, P. L. (2025). Wear-and corrosion-resistant coatings for extreme environments: advances, challenges, and future perspectives. Coatings, 15(8), 878.
5. Aung, H. (2007). An analysis of the study of mechanical properties and microstructural relationship of HSLA steels used in ship hulls (Publication No. 2006) [Master's dissertation, World Maritime University]. The Maritime **Commons:** Digital Repository of the World Maritime University. commons.wmu.se
6. Awad, A. H., Alsabaan, M., Ibrahem, M. I., Saraya, M. S., Elksasy, M. S. M., Ali-Eldin, A. M., & Abdelsalam, M. M. (2024). Low-cost IoT-based sensors dashboard for monitoring the state of health of mobile harbor cranes: Hardware and software description. Heliyon, 10(22).

7. Aziz, E. M., & Kodur, V. K. R. (2016). Residual strength of high-strength low-alloy ASTM A572 steel after exposure to elevated temperatures. Journal of Materials in Civil Engineering, 28(4), 04015165.
8. Callister, W. D., & Rethwisch, D. G. (2018). Materials science and engineering: An introduction (10th ed.). Wiley.
9. Geng, X., Zhang, Y., & Liu, B. (2023). Structural material longevity benchmarks for heavy-duty container handling infrastructure. Materials Performance and Characterization, 12(1), 85–99.
10. Gomaa, S., El-Din, M., & Hassan, A. (2024). Corrosion morphology and subsequent degradation of mechanical ductility in structural plate steels exposed to marine environments. Corrosion Science, 210, 111230.
11. Hrabovský, L., Demec, P., & Tkac, J. (2021). Detection of mechanical stress in bridge cranes caused by operational skewing. Mechanika, 27(2), 145–152.
12. Hrabovský, L., Schmidt, M., & Fries, T. (2021). Evaluation of operational skewing induced mechanical stresses in bridge crane frameworks using validated finite element models. Engineering Failure Analysis, 122, 105244.
13. Jinyemiema, T. K., Okachi, I., & Ariavie, G. O. (2026). Modelling of gyroscopic motion approach to peeling of cassava tubers on the basis of energy consumption. Journal of Harbin Engineering University, 47(3), 269–277.
14. Kannan, M. (2014). A Study of Microstructure, Quasi-Static Response, Fatigue, Deformation and Fracture Behavior of High Strength Alloy Steels (Doctoral dissertation, University of Akron).
15. Khanna, O. P. (2018). Material science and metallurgy. Dhanpat Rai Publications.
16. Kishore, K., Kumar, A., & Mukhopadhyay, N. K. (2020). Metallurgical failure analysis of a 24 T crane hook after extended industrial service. Case Studies in Engineering Failure Analysis, 14, 100189.
17. Lee, J. S., & Choi, S. H. (2021). Mechanical features and yield strength reduction factors of structural high-strength steels at elevated temperatures. Construction and Building Materials, 291, 123305.
18. Murray, T. M., Dinan, R. J., & Shull, J. S. (2023). Dynamic increase factors for structural steels under high strain-rate uniaxial tensile loading configurations. International Journal of Impact Engineering, 175, 104522.
19. Orobey, V., Das, A., & Banerjee, S. (2021). Boundary and finite element diagnostic modeling of gantry crane structural wall thinning under aggressive marine stressors. Marine Structures, 78, 102980.
20. Shan, S., Wang, H., & Chao, M. (2024). Optimization metrics for structural horizontal reach configurations in modern ship-to-shore container cranes. Journal of Marine Science and Application, 23(1), 44–56.

21. Sitompul, R. (2022). Operational maneuverability and structural load modeling of mobile harbour crane chassis configurations. International Journal of Mechanical Sciences, 218, 107055.
22. Tai, J. L., Hameed Sultan, M. T., Grzejda, R., & Shahar, F. S. (2025). Remote Non-Destructive Testing of Port Cranes: A Review of Vibration and Acoustic Sensors with IoT Integration. Journal of Marine Science and Engineering, 13(7), 1338.
23. Yadav, R., Mishra, P., & Upadhyay, S. (2023). Finite element mapping of real-time stress concentration patterns within multi-axial loaded crane hooks via ANSYS. International Journal of Mechanics and Solids, 18(1), 23–36.
24. Zhan, Z., Wang, Z., Shi, Z., Yang, Y., Lu, W., Wang, H., Wang, Z., Chai, F., & Luo, X.-B. (2024). Effect of chromium and molybdenum addition on the matching mechanism of strength–ductility–toughness of low carbon medium manganese steel. Journal of Materials Research and Technology.
25. Zrni ü, N., & Hoffmann, K. (2004). Development of design of ship-to-shore container cranes: 1959–2004. In International Symposium on History of Machines and Mechanisms: Proceedings HMM2004 (pp. 229-242). Dordrecht: Springer Netherlands.
26. modeling of mobile harbour crane chassis configurations. International Journal of Mechanical Sciences, 218, 107055.
27. Tai, J. L., Hameed Sultan, M. T., Grzejda, R., & Shahar, F. S. (2025). Remote Non-Destructive Testing of Port Cranes: A Review of Vibration and Acoustic Sensors with IoT Integration. Journal of Marine Science and Engineering, 13(7), 1338.
28. Yadav, R., Mishra, P., & Upadhyay, S. (2023). Finite element mapping of real-time stress concentration patterns within multi-axial loaded crane hooks via ANSYS. International Journal of Mechanics and Solids, 18(1), 23–36.
29. Zhan, Z., Wang, Z., Shi, Z., Yang, Y., Lu, W., Wang, H., Wang, Z., Chai, F., & Luo, X.-B. (2024). Effect of chromium and molybdenum addition on the matching mechanism of strength–ductility–toughness of low carbon medium manganese steel. Journal of Materials Research and Technology.
30. Zrni ü, N., & Hoffmann, K. (2004). Development of design of ship-to-shore container cranes: 1959–2004. In International Symposium on History of Machines and Mechanisms: Proceedings HMM2004 (pp. 229-242). Dordrecht: Springer Netherlands.